

Flavor triangle of the diffuse supernova neutrino background

Zahra Tabrizi and Shunsaku Horiuchi

Center for Neutrino Physics, Department of Physics, Virginia Tech,
Blacksburg, VA 24061, U.S.A.

E-mail: ztabrizi@vt.edu, horiuchi@vt.edu

Received December 21, 2020

Revised March 16, 2021

Accepted April 2, 2021

Published ???, 2021

Abstract. Although Galactic core-collapse supernovae (SNe) only happen a few times per century, every hour a vast number of explosions happen in the whole universe, emitting energy in the form of neutrinos, resulting in the diffuse supernova neutrino background (DSNB). The DSNB has not yet been detected, but Super-Kamiokande doped with gadolinium is expected to yield the first statistically significant observation within the next several years. Since the neutrinos produced at the core collapse undergo mixing during their propagation to Earth, the flavor content at detection is a test of oscillation physics. In this paper, we estimate the expected DSNB data at the DUNE, Hyper-K and JUNO experiments which when combined are sensitive to all different neutrino flavors. We determine how well the flavor content of the DSNB will be reconstructed in the future, for a Mikheyev-Smirnov-Wolfenstein (MSW) scenario as well as a neutrino decay scenario. A large fraction of the flavor space will be excluded, but the heavy-lepton neutrino flux remains a challenge.

Keywords: core-collapse supernovas, neutrino properties, supernova neutrinos

ArXiv ePrint: [2011.10933](https://arxiv.org/abs/2101.10933)

Contents

1	Introduction	1
2	DSNB flux	2
2.1	Neutrino emission models	2
2.2	DSNB formulation	4
2.3	MSW	4
2.4	Neutrino decay	6
3	DSNB rate at different detectors	7
3.1	DUNE	7
3.2	Hyper-K	8
3.3	JUNO	11
4	Results	13
5	Conclusions	16

1 Introduction

When a massive star enters the end of its life, a core collapse will happen. During this process, neutrino and anti-neutrino of all flavors are produced at the core of the newly formed proto-neutron star. These neutrinos carry away the bulk of the tremendous amount of energy liberated in the collapse ($\sim 10^{53}$ ergs), and are emitted over a period of several seconds (for reviews, see, e.g., refs. [1–7]). Eventually, the collapsed core settles to a neutron star (NS) or a black hole (BH). In the core-collapsed core, the heavy lepton neutrinos attain similar energy spectra. Therefore, the emitted neutrinos are often described by three neutrino fluxes, ν_e , $\bar{\nu}_e$ and ν_x , where the latter collectively denotes ν_μ , $\bar{\nu}_\mu$, ν_τ and $\bar{\nu}_\tau$ (but, see [8] for a possible acceleration mechanism which distinguishes ν_μ 's and ν_τ 's).

After production, the neutrinos will flavor mix on their way to Earth, through (i) collective flavor oscillation, which happens within a few hundred kilometers from the core due to $\nu - \nu$ coherent scattering [9–19], (ii) through the coherent forward scattering on electrons of the stellar matter, described by the Mikheyev-Smirnov-Wolfenstein (MSW) mechanism [20, 21], and (iii) vacuum oscillations. Even though vacuum and MSW effects are well-understood, collective oscillations are still not understood very well, even though they can drastically change the flavor-dependent neutrino fluxes. New flavor instabilities are being discovered due to spontaneously broken symmetries [22–26], and the understanding of the so-called fast conversion [27–29] is still very approximate [30]. In addition, several beyond the Standard Model physics scenarios indicate that a heavy neutrino state can decay to a lighter one [31–54], which again will alter the prediction of the flavor-dependent neutrino fluxes. Each of these scenarios indicate that different flavor content of neutrinos can reach terrestrial detectors, depending on which one is the correct one. Hence, it is of great interest to look for novel ways to test the SN neutrino flavor content. These motivate a data-driven way to identify whether the DSNB imply standard MSW or goes beyond.

Present and upcoming neutrino detectors will have the capability to probe the flavor content of SN neutrinos. For Galactic core collapse, detectors such as Super-Kamiokande (Super-K), the Deep Underground Neutrino Experiment (DUNE), and Jiangmen Underground Neutrino Observatory (JUNO) anticipate high statistics of neutrino events. These will allow to probe, e.g., the number of neutrino species [55], constrain the parameters of the neutrino decay [56] and the neutrino magnetic moment [57, 58]. Using multiple detection channels will allow flavor dependent studies. For example, the $\bar{\nu}_e$ will be reconstructed using inverse-beta decay (IBD) events, ν_e reconstructed using ν -electron scattering and/or CC on argon at DUNE, and ν_x probed using ν -proton scattering at JUNO [59–61].

However, Galactic SNe are rare, happening only a few times per century [62]. Meanwhile, every hour a vast number of explosions happen in the whole universe. The resulting neutrinos are called the diffuse supernova neutrino background (DSNB) and have energies between a few MeV up to tens of MeV (see e.g., refs. [63, 64] for recent reviews). The DSNB complements the Galactic supernova searches (and does not replace them) since it traces the mean neutrino emission; a Galactic search will need centuries to collect a reasonable sample size of core collapses. Although the DSNB has not yet been detected, the gadolinium (Gd) enrichment at Super-K, originally proposed in ref. [65], will drastically reduce the backgrounds making it possible to observe a few DSNB $\bar{\nu}_e$ events per year [66]. Furthermore, long baseline neutrino experiments which are in construction will be sensitive to different flavors of DSNB neutrinos with high statistics, e.g., Hyper Kamiokande (Hyper-K) experiment in Japan [67], the JUNO in China [68] and DUNE in the United States [69].

In this work we study the flavor structure of the DSNB, and quantify how well future neutrino detectors will determine the ratio of the flux of ν_α divided by the total flux, f_α , for different oscillation scenarios. For detectors, we consider DUNE, Hyper-K and JUNO, and we use these to find the upper/lower bounds on the flavor ratios f_α for $\alpha = \nu_e, \bar{\nu}_e$, and ν_x . We consider multiple detection channels: IBD, absorption on argon, ν -electron scattering, and ν -proton scattering. We employ different neutrino emission models and allow a generous uncertainty on the DSNB flux, and we compare the ranges of f_α adopting the MSW mechanism in the absence and presence of neutrino decay. The paper is organized as follow: in section 2, we describe the simulations used to describe the DSNB flux. In section 3, we discuss the calculation of the DSNB events at several different experiments, namely DUNE, Hyper-K and JUNO. We show our results in section 4 and finally, we make our concluding remarks in section 5.

2 DSNB flux

2.1 Neutrino emission models

For the calculation of the DSNB fluxes we employ two approaches. In the first, we adopt the predictions of ref. [70], hereafter H18, where the authors performed a detailed study combining multiple simulations of both core collapse of massive stars to neutron stars and black holes. This approach is an attempt to account for the progenitor-dependence of core-collapse neutrino emission. In the second approach, we adopt a simple Fermi-Dirac (FD) model described by a thermal temperature.

In H18, suites of axisymmetric two-dimensional hydrodynamical simulation of core collapse to neutron stars were combined with half a dozen spherically symmetric one-dimensional simulations of core collapse to black holes. For the collapse to neutron stars, the authors considered two sets of simulations: (i) a large suite of over 100 progenitors [71] using a leakage

approximation for heavy lepton neutrino transport and a more sophisticated ray-by-ray neutrino transport for ν_e and $\bar{\nu}_e$, and (ii) a smaller suite of 18 progenitors [72] using a ray-by-ray neutrino transport for all neutrino flavors. Both were also augmented by a simulation of core collapse of an ONeMg core star [73]. For the purposes of this study, we adopt the predictions based on the latter set, since we need accurate spectral information for all neutrino flavors.

Here, we briefly summarize the procedure and refer the reader to H18 for details. For each progenitor, the neutrino's spectral parameters (i.e., the total energy, mean energy, and spectral shape or pinching parameter) are obtained directly from the simulations. Since simulations cover only the first ~ 1 second after core bounce, a time extrapolation is necessary to cover the long-term neutrino emission. Such an extrapolation is not needed for collapse to black holes, since the simulations cover the time until black hole formation. The time-summed neutrino spectrum is then fit to a pinched FD functional form as [74, 75],

$$F(E) = \frac{(1 + \langle \alpha \rangle)^{(1 + \langle \alpha \rangle)}}{\Gamma(1 + \langle \alpha \rangle)} \frac{E_\nu^{\text{tot}} E^{\langle \alpha \rangle}}{\langle E_\nu \rangle^{2 + \langle \alpha \rangle}} \exp \left[- (1 + \langle \alpha \rangle) \frac{E}{\langle E_\nu \rangle} \right], \quad (2.1)$$

where E_ν^{tot} is the total neutrino energy emitted from the SNe, $\langle E_\nu \rangle$ is the mean neutrino energy and $\langle \alpha \rangle$ is a spectral shape parameter. Next, the mean neutrino spectrum $\frac{dN}{dE}$ for a population of progenitors is computed by weighting each progenitor by the initial mass function (IMF),

$$\frac{dN}{dE} = \sum_i \frac{\int_{\Delta M_i} \psi(M) dM}{\int_8^{100} \psi(M) dM} F_i(E), \quad (2.2)$$

where $\psi(M) = dn/dM$ is the IMF of stars and ΔM_i is the mass range assigned to the i th progenitor. We use a Salpeter IMF which is $\psi(M) \propto M^\eta$, where $\eta = -2.35$. The integration is performed using the solar-metallicity progenitors of ref. [76] augmented by an ONeMg core star [77, 78] to represent the mass range of core-collapse progenitors taken to be between $(8 - 100) M_\odot$.

The contribution from core collapse to black holes is uncertain due to the unknown fraction of progenitors that collapse to black holes. Theoretically, this is a complex prediction impacted by the progenitor structure, the physics of hot dense nuclear matter, as well as unsettled aspects of the SN explosion mechanism (e.g., [79–83]). However, recent observations suggest the fraction may be fairly large. For example, searches for the disappearance of massive stars [84] lead to a fraction of failed explosions of 4–43% percent at 90% C.L. [85–87], which is not only consistent with other observables but can also explain puzzles related to SNe and their remnants [88–92]. A simple procedure to include the uncertain contribution from black holes is to parametrize the fraction of stars that collapse to black holes (e.g., [93, 94]). In this work, we opt instead to adopt a fixed black hole fraction of 17% (using the parameterization of H18, this corresponds to a “critical compactness” for progenitors to collapse to black holes of $\xi_{2.5} = 0.2$) and attribute a generous uncertainty to the DSNB flux when performing our statistical forecasts.

In the second approach, we describe the mean supernova neutrino spectrum effectively by using a thermal FD distribution [64],

$$\frac{dN}{dE} = \frac{E_\nu^{\text{tot}}}{6} \frac{120}{7\pi^4} \frac{E^2}{T_\nu^4} \frac{1}{e^{E/T_\nu} + 1}, \quad (2.3)$$

where T_ν is the temperature of each neutrino flavor, $E_\nu^{\text{tot}} = 3 \times 10^{53}$ erg is the total energy liberated, and the factor 1/6 represents equipartition into the 6 neutrino and anti-neutrinos.

The temperatures can be obtained by fitting the neutrino emissions predicted by core-collapse simulations, and generally show the following hierarchy: $T_{\nu_e} < T_{\bar{\nu}_e} < T_{\nu_x}$. Compilations generally cluster around $T_{\nu_e} \approx 3\text{--}5\text{ MeV}$, $T_{\bar{\nu}_e} \approx 4\text{--}6\text{ MeV}$, and $T_{\nu_x} \approx 4\text{--}7\text{ MeV}$ [95, 96]. While this approach has often been used in the past literature, it does not take into account the progenitor dependence of the neutrino emission which is now known to be substantial [70, 97]. The benefit however is its simplicity and ease of parameterization. In the following, we therefore consider both approaches.

2.2 DSNB formulation

The DSNB differential flux is the integrated neutrino flux over redshift, appropriately weighted by the core-collapse rate, given by

$$\frac{d\phi^0}{dE} = c \int_0^{z_{\max}} R_{CC}(z) \frac{dN}{dE'} (1+z) \left| \frac{dt}{dz} \right| dz, \quad (2.4)$$

where c is the speed of light, z is the redshift, $\frac{dN}{dE'}$ is the mean neutrino spectrum per core collapse, $E' = E(1+z)$, and $|dt/dz| = H_0(1+z)[\Omega_m(1+z)^3 + \Omega_\Lambda]^{1/2}$, where $H_0 = 70 \text{ kms}^{-1}\text{Mpc}^{-1}$ is the Hubble parameter, while $\Omega_m = 0.3$ and $\Omega_\Lambda = 0.7$ are the matter and vacuum energy densities, respectively. The upper index in ϕ^0 refers to fluxes which are calculated at the source (pre-oscillation). We take $z_{\max} \equiv 5$, which is large enough to incorporate the majority of the DSNB flux. We model the cosmic history of the comoving core-collapse rate, $R_{CC}(z)$, by

$$R_{CC}(z) = \dot{\rho}^*(z) \frac{\int_8^{100} \psi(M) dM}{\int_{0.1}^{100} M \psi(M) dM} \quad (2.5)$$

where $\psi(M)$ is once again the IMF and $\rho^*(z)$ is the rate of the cosmic star formation. The cosmic star-formation rate is derived from the observed luminosity density of various star-forming priors, which are converted through use of appropriate conversion factors [98, 99]. There are various compilations of the cosmic star-formation rate and functional fits through subsets of the available data (see, e.g., [100, 101]). We adopt the smoothed piecewise form of ref. [102] (see refs. [95, 100, 102] for numerical values). While the cosmic star-formation rate has significant systematic uncertainty, one of the most dominant — the IMF — fortunately mostly cancels by performing the product with the integration ratio in eq. (2.5). The remaining uncertainty is dominated by the scatter between the measurements and is generally in the range of $\sim 20\%$ over redshifts of importance for the DSNB (see discussions in, e.g., refs. [95, 96, 100, 101]).

Figure 1 shows the differential DSNB flux as a function of the neutrino energy for ν_e , $\bar{\nu}_e$ and ν_x in orange, blue and purple, respectively. The predictions of H18 containing a black hole fraction of 17% are shown with solid curves. For comparison we also show the fluxes we have calculated using the thermal FD flux with the dashed curve, where we have chosen $T_{\nu_e} = 5\text{ MeV}$, $T_{\bar{\nu}_e} = 6\text{ MeV}$ and $T_{\nu_x} = 7\text{ MeV}$, respectively. These thermal FD fluxes are smaller than those of H18 at a few MeV but dominate above $\sim 12\text{ MeV}$, giving significantly higher neutrino rates in that region.

2.3 MSW

Once neutrinos are emitted from the neutrinospheres they will oscillate during their propagation before reaching detectors on Earth. The fluxes after oscillation are therefore a combination of the initial fluxes emitted from the neutrinospheres. During propagation through

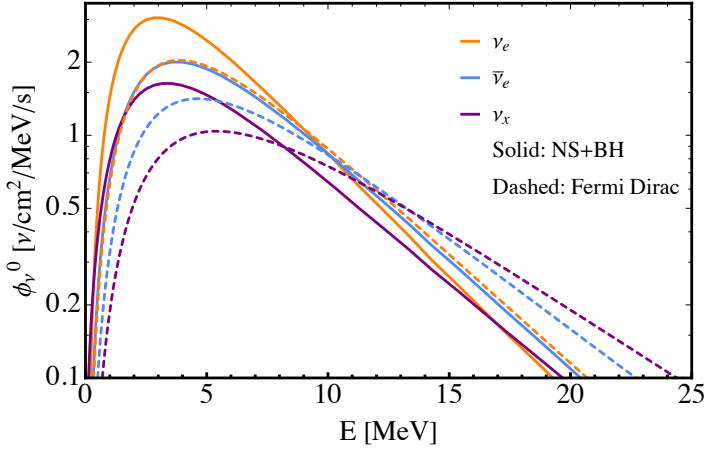


Figure 1. The DSNB flux without any oscillation effects for ν_e (orange), $\bar{\nu}_e$ (blue) and ν_x (purple) respectively. The solid curves represent the 83% neutron star plus 17% black hole (NS+BH) of H18, while the temperature dependant FD distributions are shown with dashed curves. For the thermal FD distribution we have chosen $T_{\nu_e} = 5$ MeV, $T_{\bar{\nu}_e} = 6$ MeV and $T_{\nu_x} = 7$ MeV, respectively.

the progenitor envelope, the Mikheev-Smirnov-Wolfenstein (MSW) effect becomes important due to the coherent scattering of neutrinos on electrons. Due to the matter potential, electron neutrinos ν_e will exit as ν_3 while the other states ν_x will exit as ν_1 and ν_2 , in the normal mass hierarchy (NH). In the anti-neutrino sector, electron anti-neutrinos $\bar{\nu}_e$ exit as $\bar{\nu}_1$, while $\bar{\nu}_x$ exit as $\bar{\nu}_2$ and $\bar{\nu}_3$. Therefore, we may assume the following relations between the temperatures of the flavor and mass eigenstates:

$$T_{\nu_3} = T_{\nu_e}, \quad T_{\nu_1} = T_{\nu_2} = T_{\nu_x}, \quad T_{\bar{\nu}_1} = T_{\bar{\nu}_e}, \quad T_{\bar{\nu}_2} = T_{\bar{\nu}_3} = T_{\bar{\nu}_x}, \quad (2.6)$$

again for NH. If the matter density along the neutrino trajectory varies slowly (the adiabatic propagation) then neutrinos and anti-neutrinos arrive at terrestrial detectors with the same mass eigenstate as they were in SNe, and we can write $\phi_\alpha = \sum_i |U_{\alpha i}|^2 \phi_i^0$, where U represents the Pontecorvo-Maki-Nakagawa-Sakata (PMNS) matrix. This yields the fluxes at terrestrial detectors [103, 104]

$$\phi_{\nu_e} = \phi_{\nu_x}^0, \quad (2.7)$$

$$\phi_{\bar{\nu}_e} = c_{12}^2 \phi_{\bar{\nu}_e}^0 + s_{12}^2 \phi_{\nu_x}^0, \quad (2.8)$$

$$\phi_{\nu_x} = \frac{1}{4} \left[\phi_{\nu_e}^0 + s_{12}^2 \phi_{\bar{\nu}_e}^0 + (2 + c_{12}^2) \phi_{\nu_x}^0 \right] \quad (2.9)$$

for the normal hierarchy (NH) and

$$\phi_{\nu_e} = s_{12}^2 \phi_{\nu_e}^0 + c_{12}^2 \phi_{\nu_x}^0, \quad (2.10)$$

$$\phi_{\bar{\nu}_e} = \phi_{\nu_x}^0, \quad (2.11)$$

$$\phi_{\nu_x} = \frac{1}{4} \left[c_{12}^2 \phi_{\nu_e}^0 + \phi_{\bar{\nu}_e}^0 + (2 + s_{12}^2) \phi_{\nu_x}^0 \right] \quad (2.12)$$

for the inverted hierarchy (IH), where $\phi_{\nu_\alpha}^0$ is the initial flux of (anti)neutrino flavor ν_α , $c_{12}^2 = 1 - s_{12}^2$ and $s_{12}^2 = 0.310$ is the solar mixing angle. In this paper we assume the NH for the mass ordering and show the results for this case. The results for the IH are very similar.

Collective flavour oscillations also occur within a few hundred kilometers from the core due to $\nu - \nu$ coherent scattering [9–19]. While these collective oscillations are currently the focus of much research, it is likely to be time dependent, meaning they will undergo some level of averaging out for the DSNB which detects the time-integrated neutrino spectrum. Also, during the late cooling phase of the protoneutron star, when some half of the neutrino emission occurs, the difference in spectra between flavors is much reduced, implying oscillation effects will not be pronounced. It has been predicted that collective neutrino oscillations would be subdominant compared to MSW and have an effect of less than $\sim 10\%$ [105]. However, the results after collective neutrino mixing, including its time and energy dependence, remain highly uncertain. Therefore, we do not include the uncertain collective neutrino oscillation effects in our analysis. Instead, we will estimate how well deviations from MSW can be probed with future datasets.

2.4 Neutrino decay

In principle massive neutrinos can decay to the lighter states. Within the SM this requires the lifetime to be larger than the age of the universe. However, neutrinos can decay faster if there are interactions beyond the standard model. We follow the decay mechanism described in ref. [106]. Taking the NH to be the correct one, the third mass eigenstate can decay to ν_1 . Hence, this can significantly change the flavor content of the DSNB flux arriving to the earth. We assume that neutrinos are Majorana states and they can interact with a massless scalar ϕ within the following Lagrangian:

$$\mathcal{L} \supset \frac{g}{2} \nu_i \nu_j \phi + \text{h.c.} \quad (2.13)$$

We are interested in the case where ν_3 with mass m_3 is produced as a left handed particle, where it can decay to ν_1 as a left handed (helicity conserving) or right handed (helicity flipping) daughter particle. In the lab frame the decay width of these two processes are the same:

$$\Gamma(E_3) = \frac{g^2 m_3^2}{32\pi E_3} = \frac{1}{E_3} \frac{m_3}{\tau_3}, \quad (2.14)$$

where τ_3 is the lifetime. We can then calculate the flux of the mass eigenstates at the Earth as:

$$\phi_{\nu_3}(E) = c \int_0^{z_{\max}} R_{CC}(z) \frac{dN_{\nu_e}}{dE'} (1+z) \left| \frac{dt}{dz} \right| e^{-\Gamma(E)\zeta(z)} dz, \quad (2.15)$$

$$\phi_{\bar{\nu}_3}(E) = c \int_0^{z_{\max}} R_{CC}(z) \frac{dN_{\nu_x}}{dE'} (1+z) \left| \frac{dt}{dz} \right| e^{-\Gamma(E)\zeta(z)} dz, \quad (2.16)$$

$$\phi_{\nu_1}(E) = \phi_{\nu_x}^0(E) + \int_0^{z_{\max}} dz \frac{1}{H(z)} \int_{E'}^{\infty} dE_3 \Gamma(E_3) \left[\frac{d\phi_{\bar{\nu}_3}}{dE_3} \psi_{h.c.}(E_3, E') + \frac{d\phi_{\nu_3}}{dE_3} \psi_{h.f.}(E_3, E') \right],$$

$$\phi_{\bar{\nu}_1}(E) = \phi_{\bar{\nu}_e}^0(E) + \int_0^{z_{\max}} dz \frac{1}{H(z)} \int_{E'}^{\infty} dE_3 \Gamma(E_3) \left[\frac{d\phi_{\nu_3}}{dE_3} \psi_{h.c.}(E_3, E') + \frac{d\phi_{\bar{\nu}_3}}{dE_3} \psi_{h.f.}(E_3, E') \right],$$

where $\zeta(z) = \int_0^z dz' H^{-1}(z')(1+z')^{-2}$, we have $E' = E(1+z)$ and $\phi_{\nu_\alpha}^0$ expressions are given in eq. (2.4). The other mass eigenstates are unaffected by the decay, e.g., $\phi_{\nu_2}(E) = \phi_{\nu_x}^0(E)$. Finally, the energy distribution of the daughter particle for the helicity conserving and helicity flipping cases are given by

$$\psi_{h.c.}(E_3, E_1) = \frac{2E_1}{E_3^2}, \quad \psi_{h.f.}(E_3, E_1) = \frac{2}{E_3} \left(1 - \frac{E_1}{E_3} \right). \quad (2.17)$$

Experiment	Fiducial Mass (kt)	Targets	Energy range (MeV)	efficiency
DUNE	40	6.02×10^{32}	19 – 32	86%
Hyper-K (IBD)	374	2.50×10^{34}	12 – 24	67%
Hyper-K ($\nu - e$)	374	1.25×10^{35}	10 – 20	100%
JUNO (IBD)	17	1.21×10^{33}	10 – 22	50%
JUNO ($\nu - p$)	17	1.21×10^{33}	0.2 – 1.5	100%

Table 1. Summary of the detectors set-up and values assumed in our calculations.

By inclusion of the neutrino decay the flux of ν_α at the earth changes dramatically. In this case the spectrum of different flavors at the earth for the NH are given by:

$$\begin{aligned}\phi_{\nu_e}^{\text{decay}} &= c_{12}^2 \phi_{\nu_1} + s_{12}^2 \phi_{\nu_2}, \\ \phi_{\bar{\nu}_e}^{\text{decay}} &= c_{12}^2 \phi_{\bar{\nu}_1} + s_{12}^2 \phi_{\bar{\nu}_2}, \\ \phi_{\nu_x}^{\text{decay}} &= \frac{1}{4} [s_{12}^2 (\phi_{\nu_1} + \phi_{\bar{\nu}_1}) + c_{12}^2 (\phi_{\nu_2} + \phi_{\bar{\nu}_2}) + \phi_{\nu_3} + \phi_{\bar{\nu}_3}],\end{aligned}\quad (2.18)$$

where similar expressions can be obtained for the IH case.

One can be sensitive to neutrino decay of $\tau/m \sim 10^5$ s/eV from the neutronization burst of galactic SN [107]. The DSNB however, due to the further distances, can be sensitive to the neutrino lifetimes of $\tau/m \sim 10^{10}$ s/eV. It was shown in ref. [106] that using the data of Hyper-K doped with Gd as well as THEIA one can reach a 3σ sensitivity of $\tau_3/m_3 \lesssim 5 \times 10^9$ after 20 years of data taking. Ref. [108] has also studied DSNB neutrino decay, but they have found one order of magnitude smaller sensitivity.

3 DSNB rate at different detectors

Since the DSNB flux is extremely small and only concentrates around a few MeV, enormous neutrino detectors with the ability to distinguish between the DSNB and different sources of relevant background are needed. The next generation neutrino experiments are expected to be able to deliver this. In this work we consider three different experiments which each will detect different DSNB flavors: DUNE will detect ν_e through the CC interaction on liquid Argon (LAr) while Hyper-K and JUNO will be sensitive to $\bar{\nu}_e$ through the IBD scattering. The sensitivity to heavy lepton neutrinos is more limited, but the elastic neutrino electron scattering channel at Hyper-K will be a source for detecting the sum of all flavors. Furthermore, sensitivity exists through proton scattering at JUNO, provided backgrounds can be sufficiently mitigated. The next subsections are devoted to the experimental details of each of these detectors. We list the experimental details in table 1.

3.1 DUNE

Using the LAr detector of DUNE, we will be able to detect the electron component of the DSNB flux via the CC interaction $\nu_e + Ar \rightarrow e^- + K^+$ [69]. The signature of this process is observing an electron accompanied by the decay products of the excited K^* . The DUNE far detector which has a fiducial mass of at least 40 kt will be sensitive to DSNB neutrinos from around 5 MeV to a few tens of MeV. The main sources of background at this energy are the solar hep neutrinos which have an endpoint of 18.8 MeV, and the atmospheric flux

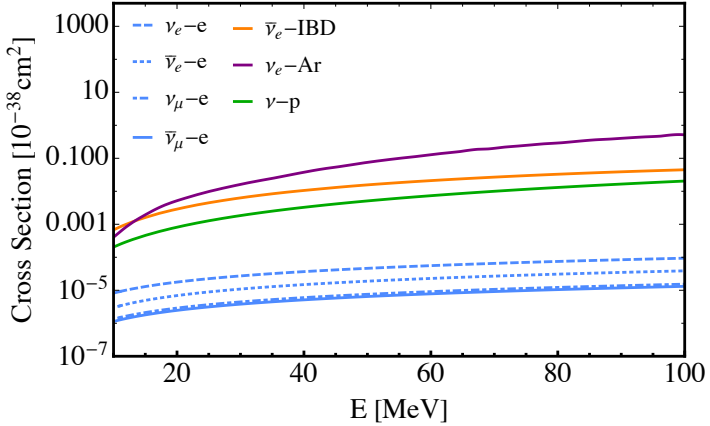


Figure 2. The cross sections as a function of the neutrino energy for the IBD scattering of $\bar{\nu}_e$ (orange), the CC ν_e scattering on Argon (purple) and the neutrino-proton elastic scattering (green). The elastic scattering of different neutrino flavors on electron are also shown in blue.

of electron neutrinos which rises in an energy around 40 MeV. Since the exact details of the DSNB backgrounds at DUNE are still under investigation, we assume DUNE will have a background similar to ICARUS [94, 109]. We calculate the events in the range of 19–31 MeV to get rid of these backgrounds. We take the CC cross section of neutrinos on Argon from ref. [69] which we have shown in figure 2.

The number of expected DSNB events at the DUNE far detector is calculated by

$$N_i^{\text{DUNE}} = n_{\text{DUNE}} \times T \times \epsilon \int_i \frac{d\phi_{\nu_e}}{dE} \sigma(E) dE \quad (3.1)$$

where n_{DUNE} is the total number of Argon targets at the detector mass and T is the total lifetime of the experiment. The fiducial mass of the far detector is 40 kt and we consider 20 years of data taking. Therefore, we have

$$n_{\text{DUNE}} = 6.02 \times 10^{32}. \quad (3.2)$$

Using this factor and assuming a detector efficiency of $\epsilon = 86\%$ [69] we find a total of 15 and 38 ν_e events with the H18 and thermal FD fluxes, respectively. Figure 3 shows the expected number of events as a function of the neutrino energy for the two different neutrino emission models. For the thermal FD flux we have chosen $T_{\nu_e} = 5$ MeV, $T_{\bar{\nu}_e} = 6$ MeV and $T_{\nu_x} = 7$ MeV, respectively. As can be seen, these temperatures result in much higher expected events than H18, even beyond the variability of the flux within its possible uncertainty. This is consistent with our choice of temperature which are on the large end of those predicted by simulations. For comparison, in the right panel we show the event rates for the decay scenario assuming different values for τ_3/m_3 , all for the H18 model. The shorter the lifetime, the faster the decay, and hence the higher the ν_1 flux and higher the ν_e events on Earth; indeed, this is what we see in figure 3.

3.2 Hyper-K

The Hyper-K experiment in Japan, which is the successor of the Super-K experiment, will be able to detect SN neutrinos down to ~ 3 MeV [67], although the threshold for the DSNB will be higher owing to backgrounds. It consists of two modules, each with a fiducial mass of

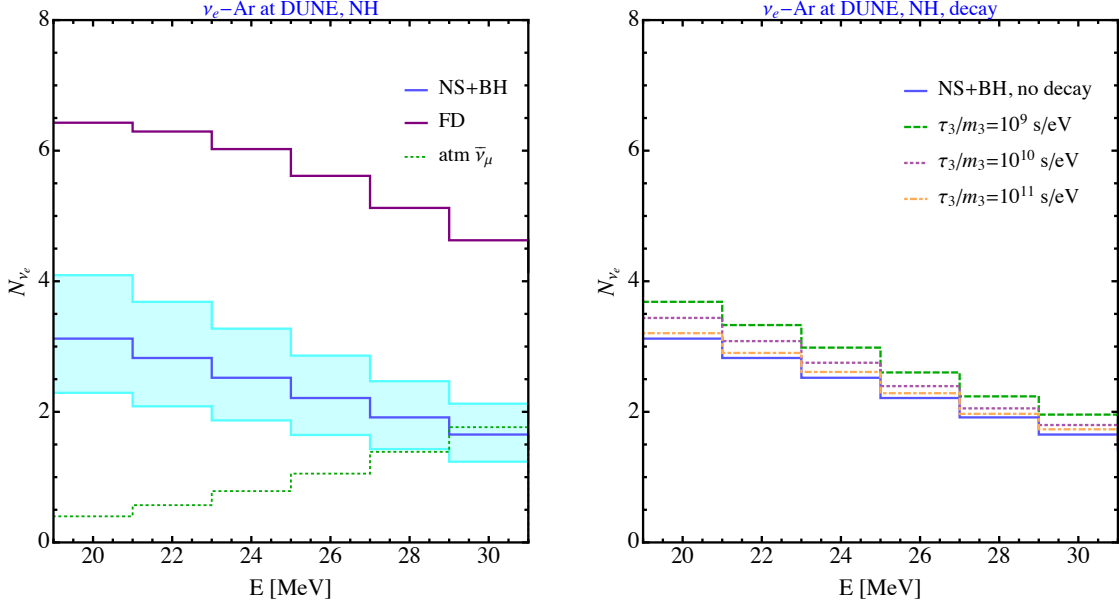


Figure 3. Expected DSNB event rates as a function of the neutrino energy at the DUNE. Left panel: the rates for the NS+BH model of H18 and the thermal FD model are shown in dark blue and purple, respectively. For the thermal FD model we have chosen temperatures of $T_{\nu_e} = 5$ MeV, $T_{\bar{\nu}_e} = 6$ MeV and $T_{\nu_x} = 7$ MeV, respectively. The light blue band shows the variability of the H18 flux within the theoretical uncertainties described in section 2.2. The background is shown in dotted green curve. Right panel: comparison of the event rates for the H18 model considering MSW scenario without decay and with decay for different values of τ_3/m_3 .

187 kt. With a combined volume of 374 kt, Hyper-K will be sixteen times larger than Super-K, resulting in great sensitivity to the DSNB. Unlike the DUNE which will be sensitive to electron neutrinos, Hyper-K will detect $\bar{\nu}_e$ neutrinos through IBD scattering $\bar{\nu}_e + p \rightarrow e^+ + n$. We get the IBD cross section from refs. [110, 111] (see figure 2).

If Hyper-K is enriched with gadolinium (Gd) its sensitivity to DSNB events will be significantly improved due to the significantly reduced backgrounds. The CC atmospheric neutrinos and the lithium-9 spallation are subdominant backgrounds at energies around tens of MeV. On the other hand, the neutral current (NC) atmospheric neutrinos which are induced due to the γ -rays produced by the NC quasi elastic scattering, are non-negligible in this range. If we assume full tagging can be reached, we can ignore this background [94]. In practice, if the tagging efficiency will be comparable to Super-K, it will be in the 90% range. The invisible muons will be similarly suppressed by neutron tagging but given its much higher rate it will remain as the main source of background, which increases with energy. Therefore, we consider an upper bound of $E < 24$ MeV to suppress the invisible muons. The modeling of backgrounds at Hyper-K enriched with Gd is taken from [67, 94]. There are other sources of background which will not be reduced by Gd, but a cut on the energy will avoid them. The dominant background at $E < 10$ MeV is the $\bar{\nu}_e$ from reactor neutrinos, which is however suppressed at $E > 10$ MeV. Therefore, we consider the range $10 \text{ MeV} < E < 24 \text{ MeV}$.

The number of expected DSNB events through the IBD cross section at the Hyper-K detector at each bin of the positron energy is calculated by

$$N_i^{\text{HK-IBD}}(E^+) = n_{\text{HK}}^{\text{IBD}} \times T \times \epsilon \int_i \frac{d\phi_{\bar{\nu}_e}}{dE} \sigma(E^+) dE^+, \quad (3.3)$$

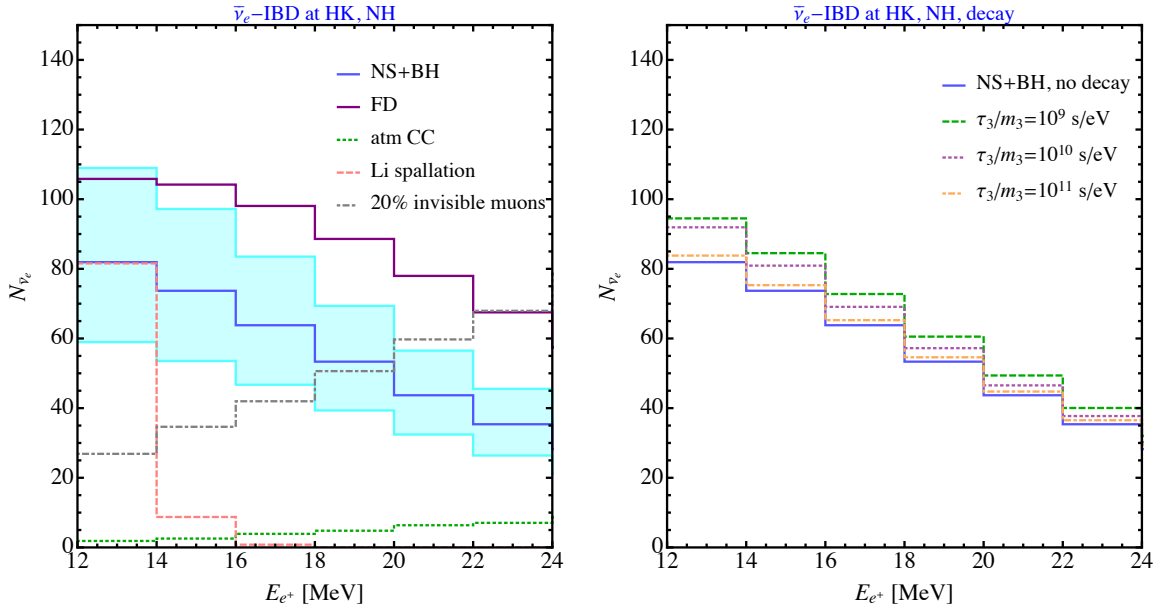


Figure 4. Expected event rates as a function of the positron energy at Hyper-K experiment for the IBD events. Left panel: the rates for the NS+BH model of H18 and the thermal FD model are shown in dark blue and purple, respectively. For the temperatures of the thermal FD flux we have chosen $T_{\nu_e} = 5$ MeV, $T_{\bar{\nu}_e} = 6$ MeV and $T_{\nu_x} = 7$ MeV, respectively. The light blue band shows the variability of the flux within the theoretical uncertainties. The backgrounds are shown in dotted green, dashed pink and dot-dashed gray curves. Right panel: comparing the event rates for the MSW scenario (no decay) with the decay mechanism for different values of τ_3/m_3 .

where we have used $E = E^+ + \Delta$ with $\Delta = 1.3$ MeV in the flux to convert the neutrino energy to the positron energy. The total number of IBD targets are $n_{\text{HK}}^{\text{IBD}} = 2.50 \times 10^{34}$. Considering a tagging efficiency of 90% and event selection efficiency of 74%, which is slightly lower than $\sim 90\%$ efficiency of the latest Super-K DSNB analysis [112], we adopt an overall detector efficiency of 67% [67]. The Hyper-K experiment will detect a total of 444 (747) $\bar{\nu}_e$ events using the H18 (thermal FD) flux. Figure 4 shows the expected number of DSNB events as a function of the positron energy compared to relevant backgrounds for Hyper-K enriched with Gd. In the right panel, we also show how different values of τ_3/m_3 can change the expected DSNB events under the decay scenario. Similar to ν_e events at DUNE, a faster neutrino decay can result in higher $\bar{\nu}_e$ events at Hyper-K.

Hyper-K can also be sensitive to the sum of all neutrino flavors due to the elastic scattering of neutrinos on electrons: $\nu + e \rightarrow \nu + e$, where the observable will be a forward going electron. Although the cross section will be almost three orders of magnitudes suppressed compared to IBD (see figure 2), in this way Hyper-K can be sensitive to ν_e and ν_x DSNB as well. The differential $\nu - e$ scattering cross section is given by [113],

$$\frac{d\sigma}{dE_R} = \frac{2G_F^2 m_e}{\pi} \left\{ g_1^2 + g_2^2 \left(1 - \frac{E_R}{E} \right)^2 - g_1 g_2 \frac{m_e E_R}{E^2} \right\}, \quad (3.4)$$

where G_F is the Fermi constant, E is the energy of the incoming neutrino, and m_e is the electron mass and E_R is its recoil kinetic energy. The couplings g_1 and g_2 for different neutrino flavors depend on the weak angle $\sin^2 \theta_w$ and are listed in table 1 of [113].

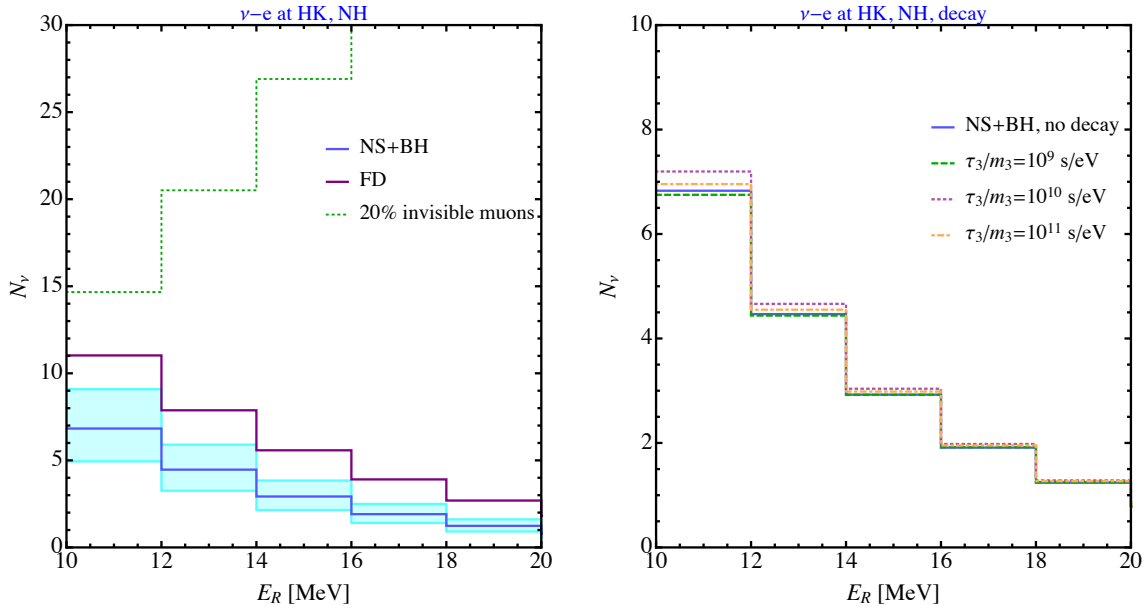


Figure 5. Expected event rates as a function of the electron recoil energy at Hyper-K experiment for the $\nu - e$ events. Color coding is the same as figure 4. The invisible muon background shown here is the same reduced rate as shown in figure 4 for clarity to show the shape of the signal, but in the analysis we use the unreduced rate.

The number of $\nu - e$ DSNB events at Hyper-K as a function of the electron recoil energy is given by

$$N_i^{\text{HK}-\nu-e}(E_R) = \sum_{\alpha=\nu_e, \bar{\nu}_e, \nu_x} n_{\text{HK}}^{\nu-e} \times T \times \epsilon \int_i dE_R \int_{E_R}^{E_R^{\max}} dE \frac{d\phi_{\nu_\alpha}}{dE} \frac{d\sigma_{\nu_\alpha}}{dE_R}, \quad (3.5)$$

where the number of electron targets is $n_{\text{HK}}^{\nu-e} = 1.25 \times 10^{35}$. Considering the recoil energy larger than 10 MeV we can get rid of the reactor neutrinos, and the solar angular cut can get rid of the solar neutrinos as the main sources of background. The invisible muons are however unavoidable, for which we show in figure 5 the results from ref. [65]. Note however that this is the reduced rate considering coincidence tagging which applies to IBD events. For $\nu - e$ events the coincidence cut does not apply, and we have to remove the background reduction factor of five. Assuming a detection efficiency of 100% above the threshold, we find that Hyper-K will be able to observe 17 (31) $\nu - e$ events using the H18 (thermal FD) flux, in the range of $10 \text{ MeV} < E_R < 20 \text{ MeV}$, but this is small compared to the invisible muon events. Thus, Hyper-K will not be able to claim standalone detection, but would constrain extremely high fluxes of ν_e and ν_x when combined with its IBD channel (and when further combined with DUNE’s measurement of ν_e , constrain high ν_x fluxes). We show in figure 5 the expected number of $\nu - e$ DSNB events at Hyper-K as a function of the electron recoil energy (left panel), as well as the comparison between the MSW with and without decays (right panel).

3.3 JUNO

The JUNO detector in China has a fiducial volume of 17 kt, made of linear alkylbenzene liquid scintillator ($\text{C}_6\text{H}_5\text{C}_{12}\text{H}_{25}$) [68]. JUNO will be able to detect $\bar{\nu}_e$ events thought IBD

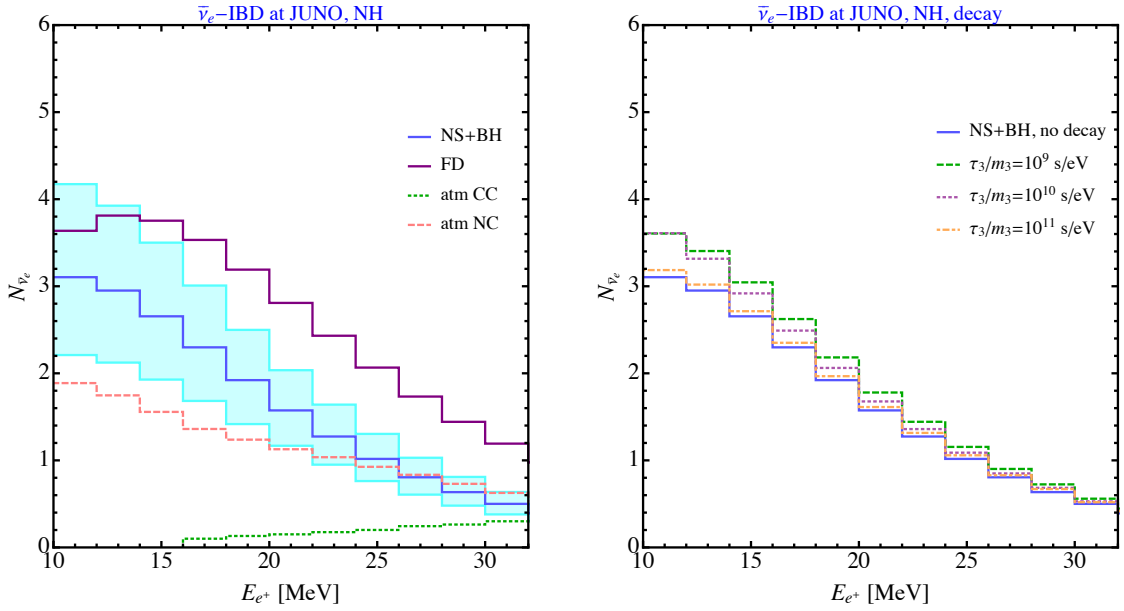


Figure 6. Number of IBD events at JUNO as a function of the positron energy. The color coding is similar to figure 4.

interaction. We calculate the number of IBD events using eq. (3.3) with $n_{\text{JUNO}}^{\text{IBD}} = 1.21 \times 10^{33}$ and a detection efficiency of 50%. The main sources of background here are the reactor electron anti-neutrinos, which we can get rid of with a cut of $E_{e^+} > 10$ MeV, and the atmospheric $\bar{\nu}_e$ events as well as the NC atmospheric, which we take from refs. [68, 94]. We show in figure 6 the expected number of IBD events at JUNO as a function of the positron energy as well as the backgrounds. In total we expect JUNO will be able to detect 19 (30) IBD events in 20 years of data taking, using the H18 (thermal FD) flux, in the range of $10 \text{ MeV} < E_{e^+} < 32 \text{ MeV}$.

In addition to the IBD detection of $\bar{\nu}_e$, JUNO can also detect neutrino events with the neutrino-proton elastic scattering which is sensitive to the sum of all neutrino flavors. In this case the differential cross section is given by [114]

$$\begin{aligned} \frac{d\sigma}{dT_{\text{ke}}} &= \frac{G_F^2 m_p}{\pi} \left\{ c_v^2 \left(1 - \frac{m_p T_{\text{ke}}}{2E^2} \right)^2 + c_a^2 \left(1 + \frac{m_p T_{\text{ke}}}{2E^2} \right)^2 \right\} \\ &= 4.83 \times 10^{-42} \frac{\text{cm}^2}{\text{MeV}} \left(1 + 466 \frac{T_{\text{ke}}}{E^2} \right), \end{aligned} \quad (3.6)$$

where m_p is the proton mass, T_{ke} is its kinetic energy, $c_v = 0.04$ and $c_a = 1.27/2$. The number of $\nu - p$ events at JUNO is given by

$$N_i^{\text{JUNO}-\nu-\text{p}}(T) = \sum_{\alpha=\nu_e, \bar{\nu}_e, \nu_x} n_{\text{JUNO}}^{\nu-\text{p}} \times T \times \epsilon \int_i dT_{\text{ke}} \int_{\sqrt{m_p T_{\text{ke}}/2}}^{T_{\text{ke}}^{\text{max}}} dE \frac{d\phi_{\nu_\alpha}}{dE} \frac{d\sigma}{dT_{\text{ke}}}, \quad (3.7)$$

where $n_{\text{JUNO}}^{\nu-\text{p}} = 1.21 \times 10^{33}$ (the same as number of IBD targets) and we assume a detection efficiency of 100%. However, this channel is a big challenge; the main difficulty is that unlike IBD where a coincidence signature suppresses backgrounds, the proton scattering appears as a single flash of light with a much higher single-event backgrounds rate [68]. The relevant

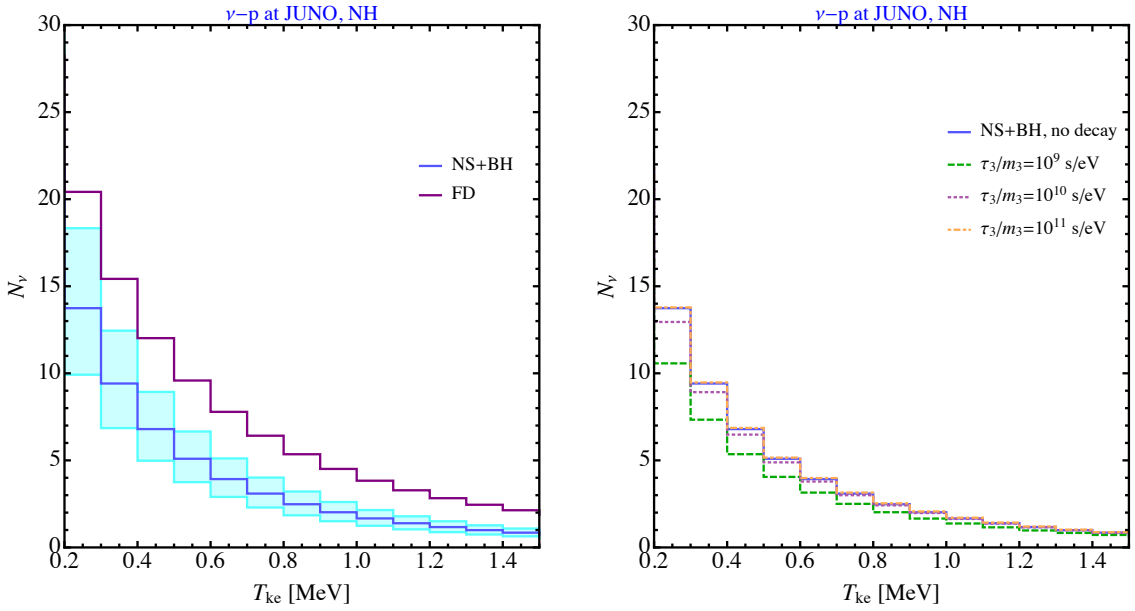


Figure 7. Number of $\nu - p$ events at JUNO as a function of the kinetic energy of proton. The color coding is the same as figure 4.

backgrounds arise from a variety of radioactive decays as well as cosmogenic backgrounds and solar neutrinos. The DSNB background in the $\nu - p$ channel of JUNO has not been studied in depth yet, and it remains to be determined how well factors such as material distillation, fiducial cuts, and pulse shape discrimination will mitigate these backgrounds [115]. As an optimistic scenario, we therefore follow the Galactic search where scintillator detectors are expected to significantly suppress background once a cut of $T_{\text{ke}} > 0.2$ MeV on the proton kinetic energy is imposed [114]. Hence, we assume this will be also the case at JUNO and calculate the events at the range $0.2 - 1.5$ MeV. We expect that JUNO will collect a total of 53 (98) $\nu - p$ events using the H18 (thermal FD) model. We show in figure 7 the distribution of events for total number of $\nu - p$ events. We will first show results without this JUNO channel, and later including this channel.

4 Results

In this section we exploit the flavor composition of the DSNB flux defining the ratio of the ν_e , $\bar{\nu}_e$ and ν_x fluxes to the total flux. To see what is the potential of the DUNE, Hyper-K, and JUNO experiments to discover the DSNB flavor content, we perform a χ^2 analysis considering the systematic uncertainties using a pull method. The goal is to see what is the flavor content using the MSW mechanism, considering the DSNB fluxes discussed in section 2, and compare it with the case where neutrino decay has happened. To do this we define the flavor parameter f_α as the ratio of the fluxes of ν_e , $\bar{\nu}_e$ and ν_x to the total flux [116], that is,

$$f_\alpha \equiv \frac{\phi_\alpha}{\sum_{\beta=\nu_e, \bar{\nu}_e, \nu_x} \phi_\beta}, \quad (4.1)$$

where ϕ_α is the flux of ν_α for either the MSW or the decay scenarios. We have checked that in the range of neutrino energies considered in our studies the energy dependence of f_α is

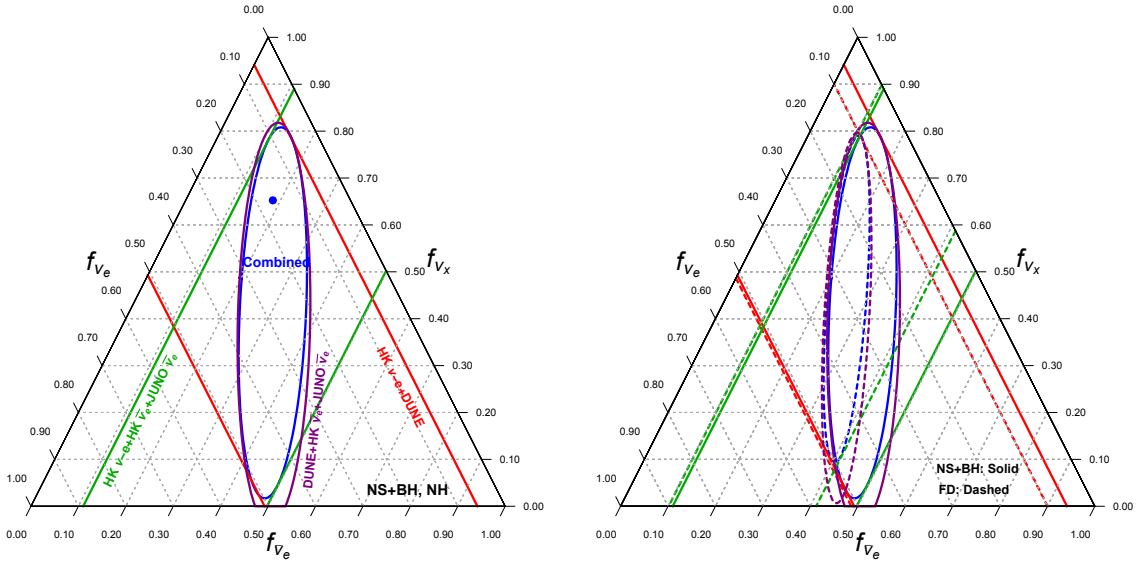


Figure 8. Flavor composition of the DSNB neutrinos at earth for the MSW scenario in NH. All the curves are at 90% C.L.. Left panel: the combined results of Hyper-K (IBD events plus $\nu - e$ events) and JUNO (IBD events) is shown in green, of Hyper-K ($\nu - e$ events) and DUNE (CC events) is shown in red, and Hyper-K (IBD events) and JUNO (IBD events) and DUNE (CC events) is shown in purple. The combined result of all four data sets are shown in blue. The blue dot shows the best fit point: $(f_{\nu_e}, f_{\bar{\nu}_e}, f_{\nu_x}) = (0.17, 0.18, 0.65)$. Right panel: the comparison of the H18 simulation (solid) with the thermal FD distribution adopting $T_{\nu_e} = 5$ MeV, $T_{\bar{\nu}_e} = 6$ MeV and $T_{\nu_x} = 7$ MeV (dashed).

less than 3%, so we assume it is a constant. We calculate the theoretical number of events at each energy bin i as $N_i^{\text{th}}(f_\alpha)$ using eqs. (3.1), (3.3), (3.5) and (3.7) but replacing the DSNB fluxes with $f_\alpha \sum_\beta \phi_\beta$. We define the χ^2 function as

$$\chi^2 = \sum_i \frac{\left((1+a)N_i^{\text{th}} + (1+b)B_i - N_i^{\text{DSNB}} - B_i \right)^2}{B_i + N_i^{\text{DSNB}}} + \frac{a^2}{\sigma_a^2} + \frac{b^2}{\sigma_b^2}, \quad (4.2)$$

where N_i^{DSNB} is the number of DSNB events at each bin i that we calculate assuming that the true theory is MSW and then the decay scenario. The background at each bin is given by B_i and is considered after all background reduction methods have been taken into account. The pull parameters a and b take into account the flux and background uncertainties, and we take their errors to be $\sigma_a = 30\%$ and $\sigma_b = 20\%$, respectively. The former is a reflection of the DSNB uncertainty, mainly driven by the uncertain core-collapse rate; while the latter is a reflection of the experimental backgrounds which depend on the detector and channel, and we assume 20% in light of the uncertainty in the low-energy (< 1 GeV) atmospheric neutrino flux [117] which contributes dominantly towards the background in most cases (including, e.g., invisible muons, atmospheric CC and NC).

We first show our results for the progenitor-averaged DSNB model of H18 with MSW mixing in the left panel of figure 8. These results are obtained without the $\nu - p$ events at JUNO. The full 3-detector 4-channel combination is shown by the blue contour, while subset combinations are shown and labeled in other colours. We find the best fit values of $(f_{\nu_e}, f_{\bar{\nu}_e}, f_{\nu_x}) = (0.17, 0.18, 0.65)$. The bound on f_{ν_e} mainly comes from the DUNE experi-

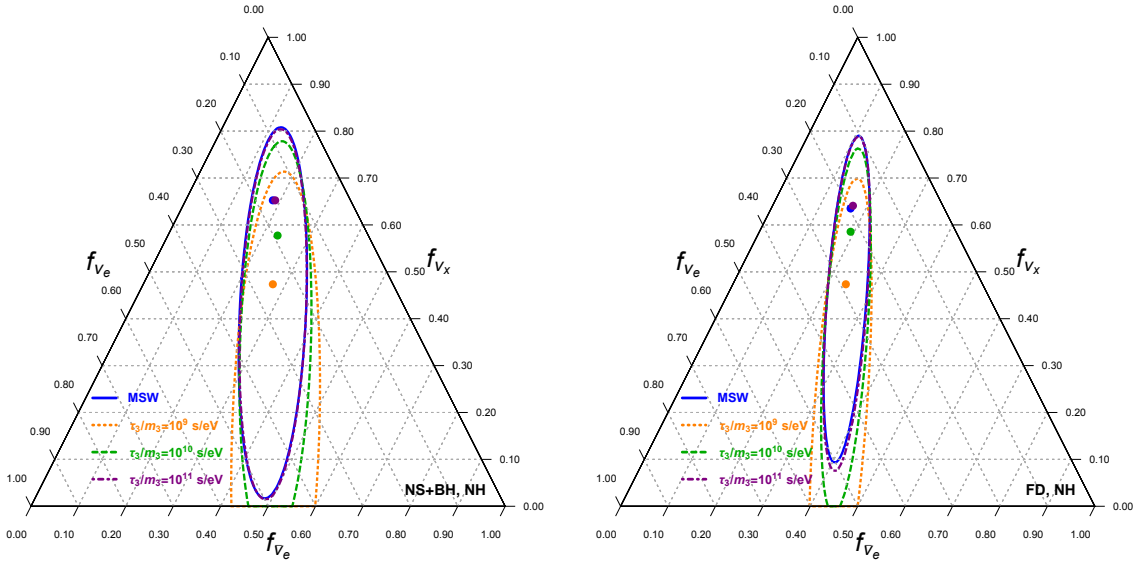


Figure 9. The 90% C.L. flavor contours for the MSW mechanism (blue) and the neutrino decay scenario for three different values of τ_3/m_3 . The left and right panels denote to the progenitor averaged H18 and thermal FD fluxes, respectively.

ment, while the IBD events at Hyper-K and JUNO give constraints on $f_{\bar{\nu}_e}$. The 90% C.L. constraints on these two parameters are

$$0.08 < f_{\nu_e} < 0.37, \quad 0.12 < f_{\bar{\nu}_e} < 0.36, \quad (4.3)$$

while the f_x is not strongly constrained. This is because the constraint on f_x comes from the $\nu - e$ events at Hyper-K, which has both low statistics and large backgrounds. The right panel of figure 8 compares the MSW scenario for the NS+BH model of H18 with the thermal FD model. As expected, the latter gives stronger constraints on the parameters due to its larger event statistics. In this case the best fit values are $(f_{\nu_e}, f_{\bar{\nu}_e}, f_{\nu_x}) = (0.19, 0.16, 0.65)$ and we find the following 90% C.L. intervals:

$$0.11 < f_{\nu_e} < 0.39, \quad 0.10 < f_{\bar{\nu}_e} < 0.32. \quad (4.4)$$

We show in figure 9 our obtained results for the neutrino decay for different values of τ_3/m_3 . As we discussed in the previous section, the faster neutrinos decay we expect higher number of ν_e and $\bar{\nu}_e$ events in terrestrial detectors. This translates into larger f_{ν_e} and $f_{\bar{\nu}_e}$, but smaller values for f_{ν_x} . This can be seen by the orange curve in figure 9 which corresponds to $\tau_3/m_3 = 10^9$ s/eV. The obtained best fit values for $(f_{\nu_e}, f_{\bar{\nu}_e}, f_{\nu_x})$ are:

$$\tau_3/m_3 = 10^9 \text{ s/eV} : (0.24, 0.27, 0.49), \quad (4.5)$$

$$\tau_3/m_3 = 10^{10} \text{ s/eV} : (0.19, 0.21, 0.60), \quad (4.5)$$

$$\tau_3/m_3 = 10^{11} \text{ s/eV} : (0.17, 0.18, 0.65). \quad (4.6)$$

If the JUNO experiment can successfully mitigate its single-background rate for the $\nu - p$ events then we can get much stronger constraints on the flavor parameters, specifically

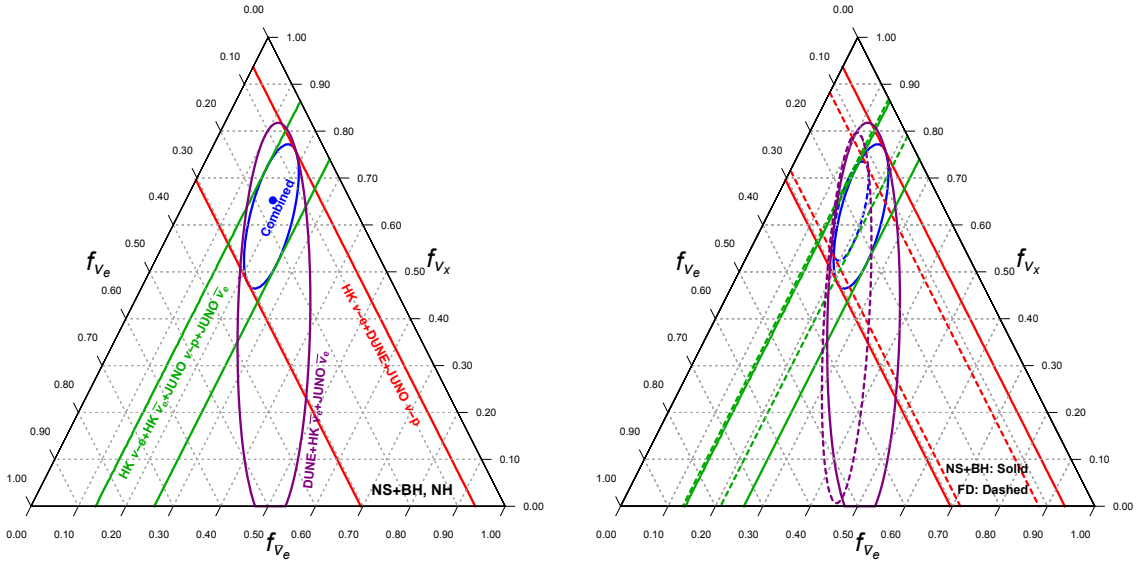


Figure 10. Same as figure 8, but the $\nu - p$ events at JUNO are also added. See text for details.

on f_{ν_x} which is largely unconstrained otherwise. We show the results in figure 10. In this case we obtain the following 90% C.L. constraints:

$$\begin{aligned} 0.08(0.11) &< f_{\nu_e} < 0.37(0.38), \\ 0.11(0.10) &< f_{\bar{\nu}_e} < 0.34(0.29), \\ 0.35(0.38) &< f_{\nu_x}. \end{aligned} \quad (4.7)$$

for the progenitor averaged H18 (thermal FD) model.

Finally, we show in figure 11 our obtained results for the neutrino decay for different values of τ_3/m_3 , including $\nu - p$ events at JUNO. The higher statistic of all different flavors at JUNO helps in getting much better sensitivity to the decay parameters, in such a way that for $\tau_3/m_3 = 10^9$ s/eV, the corresponding allowed region has very little overlap with the MSW region, and can be excluded with $\sim 90\%$ C.L..

5 Conclusions

Although Galactic SNe are rare, happening only a few times per century, each hour a vast number of SN explosions happen over the whole universe, resulting in the DSNB. With the Gd enrichment at Super-K, the first statistically significant detection of the DSNB is on the horizon over the next decade, while next generation neutrino experiments which are already under construction, like Hyper-K, DUNE and JUNO, can observe an order of magnitude or more DSNB events thanks to their enormous detectors. Just as importantly, this opens multiple detection channels with sensitivity to multiple neutrino flavors.

In this paper we studied the flavor content of the DSNB in detail using the expected DSNB events at each of the aforementioned experiments. We considered two different neutrino emission models, the first the progenitor-averaged neutron star plus black hole (NS+BH) simulation of ref. [70] (the H18 flux), and the second a simple Fermi-Dirac (FD) model described by a thermal temperature. The DSNB fluxes are compared in figure 1. If heavier

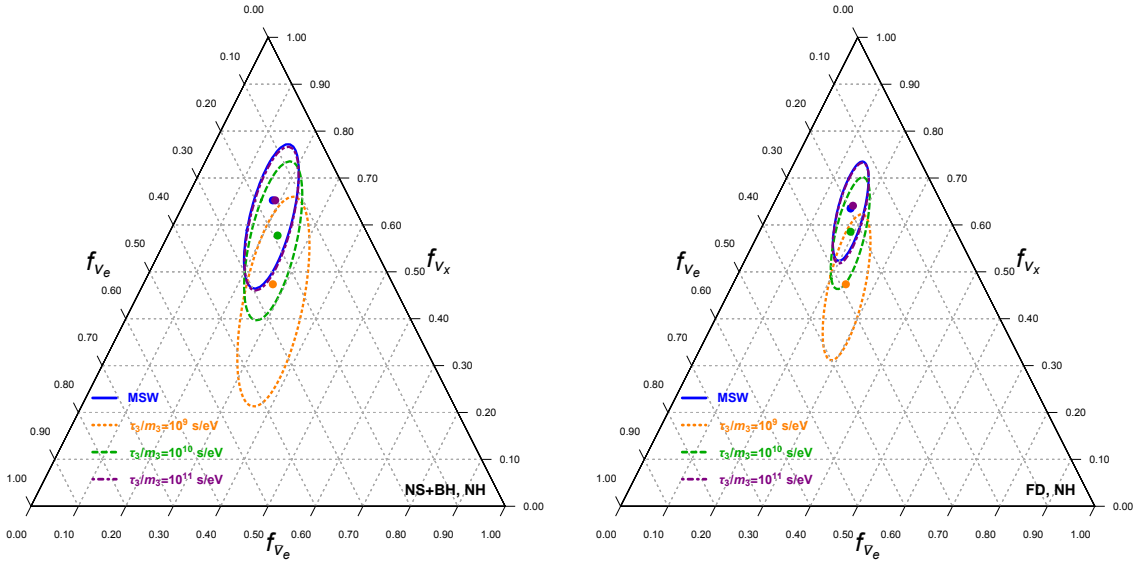


Figure 11. Same as figure 9 but including the $\nu - p$ events at JUNO. See text for details.

neutrinos decay to lighter ones, we should expect a different DSNB flavor content arriving to the Earth from the standard MSW scenario. We considered such a decay scenario, described in detail in section 2.4, and we have compared the expected event rates to the MSW mixing without decay.

The expected DSNB rates using our two DSNB models and two oscillation scenarios, for 20 years of data taking, are shown in figures 3, 4, 5, 6 and 7. In the left panels, we show the results for only MSW, while in the right panels we show results for MSW plus neutrino decay for different values of τ_3/m_3 . We have also discussed the possible background sources for each of these experiments and the methods to suppress them.

Based on our DSNB rate estimates for multiple neutrino experiments and detection channels, we study the flavor content of the DSNB using f_α , the ratio of the flux of ν_α over the total flux, at these experiments. The corresponding results are shown in figure 8, where we quantified the 90% C.L. allowed ranges for f_α comparing the progenitor-averaged NS+BH model of H18 and the thermal FD model. We find that a large fraction of the phase space will be tested out. In figure 10 we show the same, but this time including $\nu - p$ at JUNO. The $\nu - p$ at JUNO deserves a separate treatment, since it is unclear to what extent background can be mitigated, but is crucial for probing the ν_x content. Finally, we have shown the flavor triangles for the decay scenario in figures 9 and 11, with and without $\nu - p$ at JUNO, respectively. If the $\nu - p$ at JUNO can be realized, the corresponding allowed region for $\tau_3/m_3 = 10^9$ s/eV has little overlap with the no-decay MSW region, and can be excluded with $\sim 90\%$ C.L..

The DSNB is a guaranteed flux of core-collapse neutrinos which is anticipated to be detected in the next several years by Super-K enhanced by Gd. The next decades will allow detailed studies with the DSNB made possible by future neutrino experiments such as the DUNE, Hyper-K, and JUNO. The flavor content of the DSNB will be a unique component of DSNB studies in this era. We have quantified how well the flavor content of the DSNB will be constrained by 20 years of running with future detectors. As theoretical uncertainties

of the DSNB are reduced, the flavor information can become an important element to probe the physics of the DSNB.

Acknowledgments

We thank Huiling Li for fruitful discussions on JUNO backgrounds. We thank the anonymous referee for helpful comments. The work of Z.T. is supported by the U.S. Department of Energy under the award number DE-SC0020250 and DE-SC0020262. S.H. is supported by the U.S. Department of Energy Office of Science under award number DE-SC0020262 and NSF Grants Nos. AST-1908960 and PHY-1914409.

References

- [1] K. Langanke and G. Martinez-Pinedo, *Nuclear Weak Interaction Processes in Stars*, *Rev. Mod. Phys.* **75** (2003) 819 [[nucl-th/0203071](#)] [[INSPIRE](#)].
- [2] A. Mezzacappa, *Ascertaining the Core Collapse Supernova Mechanism: The State of the Art and the Road Ahead*, *Ann. Rev. Nucl. Part. Sci.* **55** (2005) 467 [[INSPIRE](#)].
- [3] K. Kotake, K. Sato and K. Takahashi, *Explosion mechanism, neutrino burst, and gravitational wave in core-collapse supernovae*, *Rept. Prog. Phys.* **69** (2006) 971 [[astro-ph/0509456](#)] [[INSPIRE](#)].
- [4] S. Woosley and T. Janka, *The physics of core-collapse supernovae*, *Nature Phys.* **1** (2005) 147 [[astro-ph/0601261](#)] [[INSPIRE](#)].
- [5] T. Foglizzo et al., *The explosion mechanism of core-collapse supernovae: progress in supernova theory and experiments*, *Publ. Astron. Soc. Austral.* **32** (2015) e009 [[arXiv:1501.01334](#)] [[INSPIRE](#)].
- [6] H.T. Janka, *Neutrino Emission from Supernovae*, [arXiv:1702.08713](#) [[INSPIRE](#)].
- [7] A. Burrows and D. Vartanyan, *Core-Collapse Supernova Explosion Theory*, *Nature* **589** (2021) 29 [[arXiv:2009.14157](#)] [[INSPIRE](#)].
- [8] H. Nagakura and K. Hotokezaka, *Non-thermal neutrinos created by shock acceleration in successful and failed core-collapse supernova*, *Mon. Not. Roy. Astron. Soc.* **502** (2021) 89 [[arXiv:2010.15136](#)] [[INSPIRE](#)].
- [9] H. Duan, G.M. Fuller, J. Carlson and Y.-Z. Qian, *Simulation of Coherent Non-Linear Neutrino Flavor Transformation in the Supernova Environment. 1. Correlated Neutrino Trajectories*, *Phys. Rev. D* **74** (2006) 105014 [[astro-ph/0606616](#)] [[INSPIRE](#)].
- [10] S. Hannestad, G.G. Raffelt, G. Sigl and Y.Y.Y. Wong, *Self-induced conversion in dense neutrino gases: Pendulum in flavour space*, *Phys. Rev. D* **74** (2006) 105010 [*Erratum ibid.* **76** (2007) 029901] [[astro-ph/0608695](#)] [[INSPIRE](#)].
- [11] G.L. Fogli, E. Lisi, A. Marrone and A. Mirizzi, *Collective neutrino flavor transitions in supernovae and the role of trajectory averaging*, *JCAP* **12** (2007) 010 [[arXiv:0707.1998](#)] [[INSPIRE](#)].
- [12] B. Dasgupta, A. Dighe, G.G. Raffelt and A.Y. Smirnov, *Multiple Spectral Splits of Supernova Neutrinos*, *Phys. Rev. Lett.* **103** (2009) 051105 [[arXiv:0904.3542](#)] [[INSPIRE](#)].
- [13] A. Esteban-Pretel, S. Pastor, R. Tomas, G.G. Raffelt and G. Sigl, *Decoherence in supernova neutrino transformations suppressed by deleptonization*, *Phys. Rev. D* **76** (2007) 125018 [[arXiv:0706.2498](#)] [[INSPIRE](#)].

[14] B. Dasgupta, A. Dighe and A. Mirizzi, *Identifying neutrino mass hierarchy at extremely small theta(13) through Earth matter effects in a supernova signal*, *Phys. Rev. Lett.* **101** (2008) 171801 [[arXiv:0802.1481](https://arxiv.org/abs/0802.1481)] [[INSPIRE](#)].

[15] B. Dasgupta, E.P. O'Connor and C.D. Ott, *The Role of Collective Neutrino Flavor Oscillations in Core-Collapse Supernova Shock Revival*, *Phys. Rev. D* **85** (2012) 065008 [[arXiv:1106.1167](https://arxiv.org/abs/1106.1167)] [[INSPIRE](#)].

[16] S. Chakraborty, R.S. Hansen, I. Izaguirre and G. Raffelt, *Self-induced flavor conversion of supernova neutrinos on small scales*, *JCAP* **01** (2016) 028 [[arXiv:1507.07569](https://arxiv.org/abs/1507.07569)] [[INSPIRE](#)].

[17] B. Dasgupta, A. Mirizzi and M. Sen, *Fast neutrino flavor conversions near the supernova core with realistic flavor-dependent angular distributions*, *JCAP* **02** (2017) 019 [[arXiv:1609.00528](https://arxiv.org/abs/1609.00528)] [[INSPIRE](#)].

[18] I. Izaguirre, G. Raffelt and I. Tamborra, *Fast Pairwise Conversion of Supernova Neutrinos: A Dispersion-Relation Approach*, *Phys. Rev. Lett.* **118** (2017) 021101 [[arXiv:1610.01612](https://arxiv.org/abs/1610.01612)] [[INSPIRE](#)].

[19] F. Capozzi, B. Dasgupta, A. Mirizzi, M. Sen and G. Sigl, *Collisional triggering of fast flavor conversions of supernova neutrinos*, *Phys. Rev. Lett.* **122** (2019) 091101 [[arXiv:1808.06618](https://arxiv.org/abs/1808.06618)] [[INSPIRE](#)].

[20] L. Wolfenstein, *Neutrino Oscillations in Matter*, *Phys. Rev. D* **17** (1978) 2369 [[INSPIRE](#)].

[21] S.P. Mikheyev and A.Y. Smirnov, *Resonance Amplification of Oscillations in Matter and Spectroscopy of Solar Neutrinos*, *Sov. J. Nucl. Phys.* **42** (1985) 913 [[INSPIRE](#)].

[22] G. Raffelt, S. Sarikas and D. de Sousa Seixas, *Axial Symmetry Breaking in Self-Induced Flavor Conversion of Supernova Neutrino Fluxes*, *Phys. Rev. Lett.* **111** (2013) 091101 [*Erratum ibid.* **113** (2014) 239903] [[arXiv:1305.7140](https://arxiv.org/abs/1305.7140)] [[INSPIRE](#)].

[23] S. Abbar, H. Duan and S. Shalgar, *Flavor instabilities in the multiangle neutrino line model*, *Phys. Rev. D* **92** (2015) 065019 [[arXiv:1507.08992](https://arxiv.org/abs/1507.08992)] [[INSPIRE](#)].

[24] S. Chakraborty, A. Mirizzi, N. Saviano and D.d.S. Seixas, *Suppression of the multi-azimuthal-angle instability in dense neutrino gas during supernova accretion phase*, *Phys. Rev. D* **89** (2014) 093001 [[arXiv:1402.1767](https://arxiv.org/abs/1402.1767)] [[INSPIRE](#)].

[25] A. Mirizzi, G. Mangano and N. Saviano, *Self-induced flavor instabilities of a dense neutrino stream in a two-dimensional model*, *Phys. Rev. D* **92** (2015) 021702 [[arXiv:1503.03485](https://arxiv.org/abs/1503.03485)] [[INSPIRE](#)].

[26] M. Zaizen et al., *Three-flavor collective neutrino conversions with multi-azimuthal-angle instability in an electron-capture supernova model*, *Phys. Rev. D* **103** (2021) 063008 [[arXiv:2011.09635](https://arxiv.org/abs/2011.09635)] [[INSPIRE](#)].

[27] R.F. Sawyer, *Speed-up of neutrino transformations in a supernova environment*, *Phys. Rev. D* **72** (2005) 045003 [[hep-ph/0503013](https://arxiv.org/abs/hep-ph/0503013)] [[INSPIRE](#)].

[28] R.F. Sawyer, *The multi-angle instability in dense neutrino systems*, *Phys. Rev. D* **79** (2009) 105003 [[arXiv:0803.4319](https://arxiv.org/abs/0803.4319)] [[INSPIRE](#)].

[29] R.F. Sawyer, *Neutrino cloud instabilities just above the neutrino sphere of a supernova*, *Phys. Rev. Lett.* **116** (2016) 081101 [[arXiv:1509.03323](https://arxiv.org/abs/1509.03323)] [[INSPIRE](#)].

[30] A. Mirizzi et al., *Supernova Neutrinos: Production, Oscillations and Detection*, *Riv. Nuovo Cim.* **39** (2016) 1 [[arXiv:1508.00785](https://arxiv.org/abs/1508.00785)] [[INSPIRE](#)].

[31] Z.G. Berezhiani, G. Fiorentini, M. Moretti and A. Rossi, *Fast neutrino decay and solar neutrino detectors*, *Z. Phys. C* **54** (1992) 581 [[INSPIRE](#)].

[32] G.L. Fogli, E. Lisi, A. Marrone and G. Scioscia, *Super-Kamiokande data and atmospheric neutrino decay*, *Phys. Rev. D* **59** (1999) 117303 [[hep-ph/9902267](https://arxiv.org/abs/hep-ph/9902267)] [[INSPIRE](#)].

[33] S. Choubey, S. Goswami and D. Majumdar, *Status of the neutrino decay solution to the solar neutrino problem*, *Phys. Lett. B* **484** (2000) 73 [[hep-ph/0004193](#)] [[INSPIRE](#)].

[34] M. Lindner, T. Ohlsson and W. Winter, *A combined treatment of neutrino decay and neutrino oscillations*, *Nucl. Phys. B* **607** (2001) 326 [[hep-ph/0103170](#)] [[INSPIRE](#)].

[35] J.F. Beacom and N.F. Bell, *Do Solar Neutrinos Decay?*, *Phys. Rev. D* **65** (2002) 113009 [[hep-ph/0204111](#)] [[INSPIRE](#)].

[36] A.S. Joshipura, E. Masso and S. Mohanty, *Constraints on decay plus oscillation solutions of the solar neutrino problem*, *Phys. Rev. D* **66** (2002) 113008 [[hep-ph/0203181](#)] [[INSPIRE](#)].

[37] A. Bandyopadhyay, S. Choubey and S. Goswami, *Neutrino decay confronts the SNO data*, *Phys. Lett. B* **555** (2003) 33 [[hep-ph/0204173](#)] [[INSPIRE](#)].

[38] J.F. Beacom, N.F. Bell and S. Dodelson, *Neutrinoless universe*, *Phys. Rev. Lett.* **93** (2004) 121302 [[astro-ph/0404585](#)] [[INSPIRE](#)].

[39] J.M. Berryman, A. de Gouv  a and D. Hernandez, *Solar Neutrinos and the Decaying Neutrino Hypothesis*, *Phys. Rev. D* **92** (2015) 073003 [[arXiv:1411.0308](#)] [[INSPIRE](#)].

[40] R. Picoreti, M.M. Guzzo, P.C. de Holanda and O.L.G. Peres, *Neutrino Decay and Solar Neutrino Seasonal Effect*, *Phys. Lett. B* **761** (2016) 70 [[arXiv:1506.08158](#)] [[INSPIRE](#)].

[41] J.A. Frieman, H.E. Haber and K. Freese, *Neutrino Mixing, Decays and Supernova Sn1987a*, *Phys. Lett. B* **200** (1988) 115 [[INSPIRE](#)].

[42] A. Mirizzi, D. Montanino and P.D. Serpico, *Revisiting cosmological bounds on radiative neutrino lifetime*, *Phys. Rev. D* **76** (2007) 053007 [[arXiv:0705.4667](#)] [[INSPIRE](#)].

[43] M.C. Gonzalez-Garcia and M. Maltoni, *Status of Oscillation plus Decay of Atmospheric and Long-Baseline Neutrinos*, *Phys. Lett. B* **663** (2008) 405 [[arXiv:0802.3699](#)] [[INSPIRE](#)].

[44] M. Maltoni and W. Winter, *Testing neutrino oscillations plus decay with neutrino telescopes*, *JHEP* **07** (2008) 064 [[arXiv:0803.2050](#)] [[INSPIRE](#)].

[45] P. Baerwald, M. Bustamante and W. Winter, *Neutrino Decays over Cosmological Distances and the Implications for Neutrino Telescopes*, *JCAP* **10** (2012) 020 [[arXiv:1208.4600](#)] [[INSPIRE](#)].

[46] C. Broggini, C. Giunti and A. Studenikin, *Electromagnetic Properties of Neutrinos*, *Adv. High Energy Phys.* **2012** (2012) 459526 [[arXiv:1207.3980](#)] [[INSPIRE](#)].

[47] L. Dorame, O.G. Miranda and J.W.F. Valle, *Invisible decays of ultra-high energy neutrinos*, *Front. in Phys.* **1** (2013) 25 [[arXiv:1303.4891](#)] [[INSPIRE](#)].

[48] R.A. Gomes, A.L.G. Gomes and O.L.G. Peres, *Constraints on neutrino decay lifetime using long-baseline charged and neutral current data*, *Phys. Lett. B* **740** (2015) 345 [[arXiv:1407.5640](#)] [[INSPIRE](#)].

[49] T. Abrah  o, H. Minakata, H. Nunokawa and A.A. Quiroga, *Constraint on Neutrino Decay with Medium-Baseline Reactor Neutrino Oscillation Experiments*, *JHEP* **11** (2015) 001 [[arXiv:1506.02314](#)] [[INSPIRE](#)].

[50] P. Coloma and O.L.G. Peres, *Visible neutrino decay at DUNE*, [arXiv:1705.03599](#) [[INSPIRE](#)].

[51] S. Choubey, D. Dutta and D. Pramanik, *Invisible neutrino decay in the light of NOvA and T2K data*, *JHEP* **08** (2018) 141 [[arXiv:1805.01848](#)] [[INSPIRE](#)].

[52] P.F. de Salas, S. Pastor, C.A. Ternes, T. Thakore and M. T  rtola, *Constraining the invisible neutrino decay with KM3NeT-ORCA*, *Phys. Lett. B* **789** (2019) 472 [[arXiv:1810.10916](#)] [[INSPIRE](#)].

[53] P.B. Denton and I. Tamborra, *Invisible Neutrino Decay Could Resolve IceCube's Track and Cascade Tension*, *Phys. Rev. Lett.* **121** (2018) 121802 [[arXiv:1805.05950](#)] [[INSPIRE](#)].

[54] A. Abdullahi and P.B. Denton, *Visible Decay of Astrophysical Neutrinos at IceCube*, *Phys. Rev. D* **102** (2020) 023018 [[arXiv:2005.07200](https://arxiv.org/abs/2005.07200)] [[INSPIRE](#)].

[55] G.G. Raffelt and S. Zhou, *Supernova bound on keV-mass sterile neutrinos reexamined*, *Phys. Rev. D* **83** (2011) 093014 [[arXiv:1102.5124](https://arxiv.org/abs/1102.5124)] [[INSPIRE](#)].

[56] S. Ando, *Appearance of neutronization peak and decaying supernova neutrinos*, *Phys. Rev. D* **70** (2004) 033004 [[hep-ph/0405200](https://arxiv.org/abs/hep-ph/0405200)] [[INSPIRE](#)].

[57] A.B. Balantekin, C. Volpe and J. Welzel, *Impact of the Neutrino Magnetic Moment on Supernova *r*-process Nucleosynthesis*, *JCAP* **09** (2007) 016 [[arXiv:0706.3023](https://arxiv.org/abs/0706.3023)] [[INSPIRE](#)].

[58] A. de Gouv  a and S. Shalgar, *Effect of Transition Magnetic Moments on Collective Supernova Neutrino Oscillations*, *JCAP* **10** (2012) 027 [[arXiv:1207.0516](https://arxiv.org/abs/1207.0516)] [[INSPIRE](#)].

[59] K. Scholberg, *Supernova Neutrino Detection*, *Ann. Rev. Nucl. Part. Sci.* **62** (2012) 81 [[arXiv:1205.6003](https://arxiv.org/abs/1205.6003)] [[INSPIRE](#)].

[60] H.-L. Li, Y.-F. Li, M. Wang, L.-J. Wen and S. Zhou, *Towards a complete reconstruction of supernova neutrino spectra in future large liquid-scintillator detectors*, *Phys. Rev. D* **97** (2018) 063014 [[arXiv:1712.06985](https://arxiv.org/abs/1712.06985)] [[INSPIRE](#)].

[61] H.-L. Li, X. Huang, Y.-F. Li, L.-J. Wen and S. Zhou, *Model-independent approach to the reconstruction of multiflavor supernova neutrino energy spectra*, *Phys. Rev. D* **99** (2019) 123009 [[arXiv:1903.04781](https://arxiv.org/abs/1903.04781)] [[INSPIRE](#)].

[62] K. Rozwadowska, F. Vissani and E. Cappellaro, *On the rate of core collapse supernovae in the milky way*, *New Astron.* **83** (2021) 101498 [[arXiv:2009.03438](https://arxiv.org/abs/2009.03438)] [[INSPIRE](#)].

[63] C. Lunardini, *Diffuse supernova neutrinos at underground laboratories*, *Astropart. Phys.* **79** (2016) 49 [[arXiv:1007.3252](https://arxiv.org/abs/1007.3252)] [[INSPIRE](#)].

[64] J.F. Beacom, *The Diffuse Supernova Neutrino Background*, *Ann. Rev. Nucl. Part. Sci.* **60** (2010) 439 [[arXiv:1004.3311](https://arxiv.org/abs/1004.3311)] [[INSPIRE](#)].

[65] J.F. Beacom and M.R. Vagins, *GADZOOKS! Anti-neutrino spectroscopy with large water Cherenkov detectors*, *Phys. Rev. Lett.* **93** (2004) 171101 [[hep-ph/0309300](https://arxiv.org/abs/hep-ph/0309300)] [[INSPIRE](#)].

[66] SUPER-KAMIOKANDE collaboration, *Supernova Relic Neutrino Search with Neutron Tagging at Super-Kamiokande-IV*, *Astropart. Phys.* **60** (2015) 41 [[arXiv:1311.3738](https://arxiv.org/abs/1311.3738)] [[INSPIRE](#)].

[67] HYPER-KAMIOKANDE collaboration, *Hyper-Kamiokande Design Report*, [arXiv:1805.04163](https://arxiv.org/abs/1805.04163) [[INSPIRE](#)].

[68] JUNO collaboration, *Neutrino Physics with JUNO*, *J. Phys. G* **43** (2016) 030401 [[arXiv:1507.05613](https://arxiv.org/abs/1507.05613)] [[INSPIRE](#)].

[69] DUNE collaboration, *Deep Underground Neutrino Experiment (DUNE), Far Detector Technical Design Report, Volume II: DUNE Physics*, [arXiv:2002.03005](https://arxiv.org/abs/2002.03005) [[INSPIRE](#)].

[70] S. Horiuchi et al., *Diffuse supernova neutrino background from extensive core-collapse simulations of 8-100M_{  } progenitors*, *Mon. Not. Roy. Astron. Soc.* **475** (2018) 1363 [[arXiv:1709.06567](https://arxiv.org/abs/1709.06567)] [[INSPIRE](#)].

[71] K. Nakamura, T. Takiwaki, T. Kuroda and K. Kotake, *Systematic Features of Axisymmetric Neutrino-Driven Core-Collapse Supernova Models in Multiple Progenitors*, *Publ. Astron. Soc. Jap.* **67** (2015) 107 [[arXiv:1406.2415](https://arxiv.org/abs/1406.2415)] [[INSPIRE](#)].

[72] A. Summa, F. Hanke, H.-T. Janka, T. Melson, A. Marek and B. M  ller, *Progenitor-dependent Explosion Dynamics in Self-consistent, Axisymmetric Simulations of Neutrino-driven Core-collapse Supernovae*, *Astrophys. J.* **825** (2016) 6 [[arXiv:1511.07871](https://arxiv.org/abs/1511.07871)] [[INSPIRE](#)].

[73] L. Hudepohl, B. M  ller, H.T. Janka, A. Marek and G.G. Raffelt, *Neutrino Signal of Electron-Capture Supernovae from Core Collapse to Cooling*, *Phys. Rev. Lett.* **104** (2010) 251101 [*Erratum ibid.* **105** (2010) 249901] [[arXiv:0912.0260](https://arxiv.org/abs/0912.0260)] [[INSPIRE](#)].

[74] M.T. Keil, G.G. Raffelt and H.-T. Janka, *Monte Carlo study of supernova neutrino spectra formation*, *Astrophys. J.* **590** (2003) 971 [[astro-ph/0208035](#)] [[INSPIRE](#)].

[75] I. Tamborra, B. Müller, L. Hudepohl, H.-T. Janka and G. Raffelt, *High-resolution supernova neutrino spectra represented by a simple fit*, *Phys. Rev. D* **86** (2012) 125031 [[arXiv:1211.3920](#)] [[INSPIRE](#)].

[76] S.E. Woosley, A. Heger and T.A. Weaver, *The evolution and explosion of massive stars*, *Rev. Mod. Phys.* **74** (2002) 1015 [[INSPIRE](#)].

[77] K. Nomoto, *Evolution of 8–10 solar mass stars toward electron capture supernovae. I — Formation of electron-degenerate $O + Ne + Mg$ cores*, *Astrophys. J.* **277** (1984) 791.

[78] K. Nomoto, *Evolution of 8–10 solar mass stars toward electron capture supernovae. I — Collapse of an $O + Ne + Mg$ core*, *Astrophys. J.* **322** (1987) 206.

[79] E. O’Connor and C.D. Ott, *Black Hole Formation in Failing Core-Collapse Supernovae*, *Astrophys. J.* **730** (2011) 70 [[arXiv:1010.5550](#)] [[INSPIRE](#)].

[80] M. Ugliano, H.T. Janka, A. Marek and A. Arcones, *Progenitor-Explosion Connection and Remnant Birth Masses for Neutrino-Driven Supernovae of Iron-Core Progenitors*, *Astrophys. J.* **757** (2012) 69 [[arXiv:1602.06327](#)] [[INSPIRE](#)].

[81] T. Ertl, H.T. Janka, S.E. Woosley, T. Sukhbold and M. Ugliano, *A two-parameter criterion for classifying the explodability of massive stars by the neutrino-driven mechanism*, *Astrophys. J.* **818** (2016) 124 [[arXiv:1503.07522](#)] [[INSPIRE](#)].

[82] T. Sukhbold, T. Ertl, S.E. Woosley, J.M. Brown and H.T. Janka, *Core-Collapse Supernovae from 9 to 120 Solar Masses Based on Neutrino-powered Explosions*, *Astrophys. J.* **821** (2016) 38 [[arXiv:1510.04643](#)] [[INSPIRE](#)].

[83] T. Ertl, S.E. Woosley, T. Sukhbold and H.T. Janka, *The Explosion of Helium Stars Evolved With Mass Loss*, [arXiv:1910.01641](#) [[INSPIRE](#)].

[84] C.S. Kochanek et al., *A Survey About Nothing: Monitoring a Million Supergiants for Failed Supernovae*, *Astrophys. J.* **684** (2008) 1336 [[arXiv:0802.0456](#)] [[INSPIRE](#)].

[85] J.R. Gerke, C.S. Kochanek and K.Z. Stanek, *The Search for Failed Supernovae with The Large Binocular Telescope: First Candidates*, *Mon. Not. Roy. Astron. Soc.* **450** (2015) 3289 [[arXiv:1411.1761](#)] [[INSPIRE](#)].

[86] S.M. Adams, C.S. Kochanek, J.R. Gerke and K.Z. Stanek, *The search for failed supernovae with the Large Binocular Telescope: constraints from 7 yr of data*, *Mon. Not. Roy. Astron. Soc.* **469** (2017) 1445 [[arXiv:1610.02402](#)] [[INSPIRE](#)].

[87] S.M. Adams, C.S. Kochanek, J.R. Gerke, K.Z. Stanek and X. Dai, *The search for failed supernovae with the Large Binocular Telescope: confirmation of a disappearing star*, *Mon. Not. Roy. Astron. Soc.* **468** (2017) 4968 [[arXiv:1609.01283](#)] [[INSPIRE](#)].

[88] S. Horiuchi, J.F. Beacom, C.S. Kochanek, J.L. Prieto, K.Z. Stanek and T.A. Thompson, *The Cosmic Core-collapse Supernova Rate does not match the Massive-Star Formation Rate*, *Astrophys. J.* **738** (2011) 154 [[arXiv:1102.1977](#)] [[INSPIRE](#)].

[89] H. Yüksel and M.D. Kistler, *The cosmic MeV neutrino background as a laboratory for black hole formation*, *Phys. Lett. B* **751** (2015) 413 [[arXiv:1212.4844](#)] [[INSPIRE](#)].

[90] C.S. Kochanek, *Failed Supernovae Explain the Compact Remnant Mass Function*, *Astrophys. J.* **785** (2014) 28 [[arXiv:1308.0013](#)] [[INSPIRE](#)].

[91] S. Horiuchi, K. Nakamura, T. Takiwaki, K. Kotake and M. Tanaka, *The red supergiant and supernova rate problems: implications for core-collapse supernova physics*, *Mon. Not. Roy. Astron. Soc.* **445** (2014) L99 [[arXiv:1409.0006](#)] [[INSPIRE](#)].

[92] C.S. Kochanek, *Constraints on Core Collapse from the Black Hole Mass Function*, *Mon. Not. Roy. Astron. Soc.* **446** (2015) 1213 [[arXiv:1407.5622](#)] [[INSPIRE](#)].

[93] C. Lunardini, *Diffuse neutrino flux from failed supernovae*, *Phys. Rev. Lett.* **102** (2009) 231101 [[arXiv:0901.0568](#)] [[INSPIRE](#)].

[94] K. Møller, A.M. Suliga, I. Tamborra and P.B. Denton, *Measuring the supernova unknowns at the next-generation neutrino telescopes through the diffuse neutrino background*, *JCAP* **05** (2018) 066 [[arXiv:1804.03157](#)] [[INSPIRE](#)].

[95] S. Horiuchi, J.F. Beacom and E. Dwek, *The Diffuse Supernova Neutrino Background is detectable in Super-Kamiokande*, *Phys. Rev. D* **79** (2009) 083013 [[arXiv:0812.3157](#)] [[INSPIRE](#)].

[96] G.J. Mathews, J. Hidaka, T. Kajino and J. Suzuki, *Supernova Relic Neutrinos and the Supernova Rate Problem: Analysis of Uncertainties and Detectability of ONeMg and Failed Supernovae*, *Astrophys. J.* **790** (2014) 115 [[arXiv:1405.0458](#)] [[INSPIRE](#)].

[97] D. Kresse, T. Ertl and H.-T. Janka, *Stellar Collapse Diversity and the Diffuse Supernova Neutrino Background*, *Astrophys. J.* **909** (2021) 169 [[arXiv:2010.04728](#)] [[INSPIRE](#)].

[98] R.C. Kennicutt Jr., *Star formation in galaxies along the Hubble sequence*, *Ann. Rev. Astron. Astrophys.* **36** (1998) 189 [[astro-ph/9807187](#)] [[INSPIRE](#)].

[99] A.M. Hopkins, *On the evolution of star forming galaxies*, *Astrophys. J.* **615** (2004) 209 [*Erratum ibid.* **654** (2007) 1175] [[astro-ph/0407170](#)] [[INSPIRE](#)].

[100] A.M. Hopkins and J.F. Beacom, *On the normalisation of the cosmic star formation history*, *Astrophys. J.* **651** (2006) 142 [[astro-ph/0601463](#)] [[INSPIRE](#)].

[101] P. Madau and M. Dickinson, *Cosmic Star Formation History*, *Ann. Rev. Astron. Astrophys.* **52** (2014) 415 [[arXiv:1403.0007](#)] [[INSPIRE](#)].

[102] H. Yüksel, M.D. Kistler, J.F. Beacom and A.M. Hopkins, *Revealing the High-Redshift Star Formation Rate with Gamma-Ray Bursts*, *Astrophys. J. Lett.* **683** (2008) L5 [[arXiv:0804.4008](#)] [[INSPIRE](#)].

[103] A.S. Dighe and A.Y. Smirnov, *Identifying the neutrino mass spectrum from the neutrino burst from a supernova*, *Phys. Rev. D* **62** (2000) 033007 [[hep-ph/9907423](#)] [[INSPIRE](#)].

[104] J.-S. Lu, Y.-F. Li and S. Zhou, *Getting the most from the detection of Galactic supernova neutrinos in future large liquid-scintillator detectors*, *Phys. Rev. D* **94** (2016) 023006 [[arXiv:1605.07803](#)] [[INSPIRE](#)].

[105] S. Chakraborty, S. Choubey, B. Dasgupta and K. Kar, *Effect of Collective Flavor Oscillations on the Diffuse Supernova Neutrino Background*, *JCAP* **09** (2008) 013 [[arXiv:0805.3131](#)] [[INSPIRE](#)].

[106] A. De Gouvêa, I. Martinez-Soler, Y.F. Perez-Gonzalez and M. Sen, *Fundamental physics with the diffuse supernova background neutrinos*, *Phys. Rev. D* **102** (2020) 123012 [[arXiv:2007.13748](#)] [[INSPIRE](#)].

[107] A. de Gouvêa, I. Martinez-Soler and M. Sen, *Impact of neutrino decays on the supernova neutronization-burst flux*, *Phys. Rev. D* **101** (2020) 043013 [[arXiv:1910.01127](#)] [[INSPIRE](#)].

[108] G.L. Fogli, E. Lisi, A. Mirizzi and D. Montanino, *Three generation flavor transitions and decays of supernova relic neutrinos*, *Phys. Rev. D* **70** (2004) 013001 [[hep-ph/0401227](#)] [[INSPIRE](#)].

[109] A.G. Cocco, A. Ereditato, G. Fiorillo, G. Mangano and V. Pettorino, *Supernova relic neutrinos in liquid argon detectors*, *JCAP* **12** (2004) 002 [[hep-ph/0408031](#)] [[INSPIRE](#)].

[110] P. Vogel and J.F. Beacom, *Angular distribution of neutron inverse beta decay*, $\bar{\nu}_e + p \rightarrow e^+ + n$, *Phys. Rev. D* **60** (1999) 053003 [[hep-ph/9903554](#)] [[INSPIRE](#)].

- [111] A. Strumia and F. Vissani, *Precise quasielastic neutrino/nucleon cross-section*, *Phys. Lett. B* **564** (2003) 42 [[astro-ph/0302055](#)] [[INSPIRE](#)].
- [112] SUPER-KAMIOKANDE collaboration, *Supernova Relic Neutrino Search at Super-Kamiokande*, *Phys. Rev. D* **85** (2012) 052007 [[arXiv:1111.5031](#)] [[INSPIRE](#)].
- [113] A. de Gouv  a, P.A.N. Machado, Y.F. Perez-Gonzalez and Z. Tabrizi, *Measuring the Weak Mixing Angle in the DUNE Near Detector Complex*, *Phys. Rev. Lett.* **125** (2020) 051803 [[arXiv:1912.06658](#)] [[INSPIRE](#)].
- [114] B. Dasgupta and J.F. Beacom, *Reconstruction of supernova ν_μ , ν_τ , anti- ν_μ , and anti- ν_τ neutrino spectra at scintillator detectors*, *Phys. Rev. D* **83** (2011) 113006 [[arXiv:1103.2768](#)] [[INSPIRE](#)].
- [115] H. Li. personal communication.
- [116] C.A. Arg  elles, T. Katori and J. Salvado, *New Physics in Astrophysical Neutrino Flavor*, *Phys. Rev. Lett.* **115** (2015) 161303 [[arXiv:1506.02043](#)] [[INSPIRE](#)].
- [117] M. Honda, T. Kajita, K. Kasahara and S. Midorikawa, *Calculation of the flux of atmospheric neutrinos*, *Phys. Rev. D* **52** (1995) 4985 [[hep-ph/9503439](#)] [[INSPIRE](#)].